Molecular Crystals and Liquid Crystals

Publication details, including instructions for authors and subscription information:
http://www.tandfonline.com/loi/gmcl20

Molecular Dynamics Simulations of Various Branched Polymeric Liquid Crystals

J. M. Ilnytskyi [a b], D. Neher [b], M. Saphiannikova [c], M. R. Wilson [d] & L. M. Stimson [e]

[a] Institute for Condensed Matter Physics, Lviv, Ukraine

[b] University of Potsdam, Potsdam, Germany

[c] Leibnitz Institute of Polymer Research, Dresden, Germany

[d] University of Durham, Durham, UK

[e] University of Western Ontario, London (ON), Canada

Version of record first published: 06 Jul 2012

To cite this article: J. M. Ilnytskyi, D. Neher, M. Saphiannikova, M. R. Wilson & L. M. Stimson (2008): Molecular Dynamics Simulations of Various Branched Polymeric Liquid Crystals, Molecular Crystals and Liquid Crystals, 496:1, 186-201

To link to this article: http://dx.doi.org/10.1080/15421400802451675

Mol. Cryst. Liq. Cryst., Vol. 496, pp. 186–201, 2008

ISSN: 1542-1406 print/1563-5287 online
DOI: 10.1080/15421400802451675

Taylor & Francis
Taylor & Francis Group

Molecular Dynamics Simulations of Various Branched Polymeric Liquid Crystals

J. M. Ilnytskyi[1,2], D. Neher[2], M. Saphiannikova[3], M. R. Wilson[4], and L. M. Stimson[5]
[1]Institute for Condensed Matter Physics, Lviv, Ukraine
[2]University of Potsdam, Potsdam, Germany
[3]Leibnitz Institute of Polymer Research, Dresden, Germany
[4]University of Durham, Durham, UK
[5]University of Western Ontario, London (ON), Canada

We discuss molecular dynamics simulations for several types of polymeric liquid crystals. Dendrimers with a variety of mesogenic attachments are studied in isotropic, nematic and smectic A solvents, with an emphasize on the coupling between molecular shape and the structure of the phase. The structure and dynamics of liquid crystal side-chain polymers are studied within different bulk phases. Here, again a strong coupling is noted between molecular shape and molecular organisation within each phase. We also consider photo-induced deformation in azobenzene-containing polymers and demonstrate that the "opposite sign" of these deformations, observed experimentally in liquid crystalline and amorphous systems, can be explained solely by the reorientation of trans-isomers of azobenzene.

Keywords: azobenzene; dendrimer; molecular dynamics; side-chain polymer

1. INTRODUCTION

As with many forms of soft matter, macromolecular liquid crystals (LCs), exhibit interesting phenomena, which occur over a wide range of time and length scales. Many effects (self-organisation, phase transitions, field-driven changes of the structure) appear on a mesoscale level but their origin is often to be found at the quantum mechanical level [1]. Classical computer simulations are known to be powerful for the study of self-organising phenomena, but their success is highly

J.I. acknowledges funding by EPSRC and by DFG grant NE 410/8-2.
Address correspondence to J. M. Ilnytskyi, Institute for Condensed Matter Physics, Lviv, Ukraine. E-mail: iln@icmp.lviv.ua, ilnytsky@uni-potsdam.de

dependent on accurate modeling of molecular interactions [2]. Covering such a broad range of times, lengths and energies is a real challenge for computer simulations. Several approaches are possible. One of these is multi-scale modeling, when the more detailed potentials (e.g., the ones obtained from *ab initio* calculations) are mapped onto some simpler forms (e.g., classical mechanical force fields) and the parameters of the latter are found from the best fitting of a set of equilibrium properties. Indeed, one can extend this process further, e.g., it is possible to perform successful mapping of classical force field potentials onto coarse-grained soft potentials suitable for Brownian dynamics or dissipative particle dynamics [3]. If done in a "proper way", the relevant chemically-detailed mechanisms can still be accounted for in a coarse-grained model in some "effective" way.

Hybrid models consisting of force field terms linking coarse-grained sites can be seen as a good compromise technique for modeling LC macromolecules. For example, polymer chains can be considered as a purely classical system of beads with harmonic bonds and bond angles. Flexibility of chains can be controlled via torsional angle barriers or simple constraints. Attached to such chains, LC (mesogenic) units can be represented as either stiff fragments made of several beads or, alternatively, as anisometric bodies (soft spherocylinders of ellipsoids). The latter approach was pioneered in Ref. [4] and a number of studies have occured since then (see, Ref. [5] and references therein). Several empirical force fields sets are available at this moment [6], including those specifically designed for LC systems [7]. These models can be studied by different simulation methods: both deterministic approaches (molecular dynamics) and stochastic modeling (Monte Carlo) can be used [3].

The aim of this study is to present some characteristic studies of macromolecular LCs performed with the aid of molecular dynamics (MD) simulations. The outline of the paper is as follows. Section 2 contains results for the simulations of a LC dendrimer in various LC solvents. In Section 3 we will concentrate on the phase diagram and properties of phases formed by a side-chain LC polymer. Section 4 contains some results of simulations of photo-induced deformations in LCs and amorphous polymers. Conclusions are given in Section 5.

2. MD SIMULATIONS OF A LC DENDRIMER IN ISOTROPIC, NEMATIC AND SMECTIC A SOLVENTS

Macromolecules can be seen as building blocks for the larger scale phenomena of supramolecular self-assembling [1]. In this respect, their shape and anisotropy can be the defining factor in the formation

of particular types of mesophases. Dendrimers are exotic tree-like macromolecules that can be synthesized with extremely low polydispersity and have possible future uses in several areas [8] including light harvesting and drug delivery. LC dendrimers (LCDr) can contain mesogens within a dendritic scaffold and/or on its periphery. There is strong experimental evidence for a shape-mesophase relationship for LCDrs [9], but MD simulations of these bulk phases is difficult at the present time. Some progress has been achieved using coarse-grained simulations where the dendritic scaffold is replaced by a soft sphere [10].

We performed MD simulations of generation three LCDrs in isotropic, nematic and smectic A solvents to look at how the shape of the LCDr depends on the bulk phase. Four models are considered, A, B, C, D, see Figure 1. A basic dendrimer scaffold consisting of *141* units and terminal spacers, each of *20* units, are modeled using force fields developed for linear and branched alkanes [11]. The grafted mesogenic units are

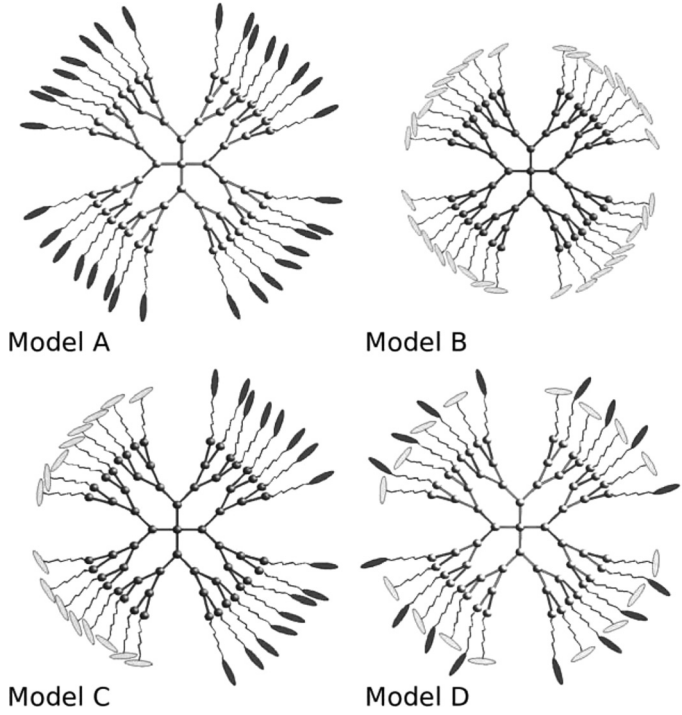

FIGURE 1 Schematic representation of four LCDrs (models A–D), branching sites are shown as balls, internal spacers as straight lines, terminally and laterally attached mesogens as ellipses, terminal spacers are shown as wavy wires.

represented as anisometric sites interacting via a Gay-Berne potential, (for further details, see Ref. [12]). The mesogenic solvent is modeled explicitly, typically using a box containing about 4500–5000 mesogenic units of the same type as those in the LCDr. MD simulations are performed with the aid of the parallel program GBMOLDD [3] in the *NVT* ensemble, with a timestep of $\Delta t = 2$ fs.

The following simulation scheme is employed [14]. The LCDr is first constructed in vacuum, then equilibrated using Monte Carlo simulations to minimize its internal energy. The solvent is equilibrated in isotropic, nematic and smectic-A phases using separate simulations. After this, two simulation boxes (the ones with the LCDr and a solvent) are combined into one box and those molecules of the solvent that overlap with the LCDr are removed. As the result, in its initial state the LCDr is placed tightly into a void cut out of the solvent. The simulations are performed for at least 4 ns, which was found to be sufficient for equilibration of the solution. Due to microphase segregation of polymer and LC subsystems, the dendritic scaffold is found in the form of relatively compact object but complete collapse is prohibited by its own stiffness. The arrangement of the terminal LC groups is driven by two tendencies. On the one hand, they find themselves in an anisotropic athermal solvent environment and would like to follow the phase of the solvent. On the other hand, their conformational and diffusive mobility is constrained by their attachment to the dendritic scaffold. We found that the terminal spacer used in this study is sufficiently long that the terminally attached LC groups of model A are able to follow the phase of the solvent, see Figure 2 (for the sake of

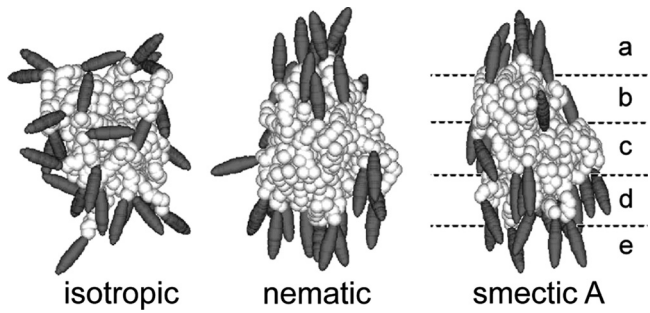

FIGURE 2 Snapshots for LCDr shape in various LC phases of the solvent, model A (polymer sites of dendritic scaffold and of terminal spacers are shown as spheres, the mesogens are shown as ellipsoids). (Revised with permission from Mark R. Wilson, Journal of Chemical Physics, 119, 3509 (2003). Copyright 2003, American Institute of Physics.)

clarity only the denrimer beads are shown). It is interesting to note that in the smectic A solvent the LC groups of the dendrimer find their places in the nearest smectic layers (indicated by a–e), while in the nematic solvent, these groups are gathered at each end of the dendrimer.

The order parameter of LCDr mesogens S_{den} in smectic A solvent grows during over a period of about 4 ns until it reaches the value of that for the solvent S_{solv}, see Figure 3, left. The shape of the LCDr is spherical in the isotropic solvent but turns to prolate along the solvent director in both nematic and smectic A phases, as seen by the behaviors of the radial disribution functions (RDF) parallel and perpendicularly to the solvent director, see Figure 3. The main effect is due to rearranging of all the beads of the generation 3 scaffold plus the beads of terminal spacers (see, *gen3 + spc* curves in Fig. 3). Here, the LCDr has sufficient flexibility within the linking chains to undergo a major molecular rearrangement in response to the weak reorientating field of the solvent. However, if the flexible chains were made shorter, the molecule would experience a frustration in terms of its inability to rearrange the mesogenic units along the solvent director, due to steric constraints within the molecule.

Problems caused by steric constraints are seen very cleary in model B, where the mesogenic units are attached laterally to the flexible chains. Contrary to model A, where mesogens are able to follow the symmetry of the bulk phase of the solvent, in model B they are forced to follow the spherical symmetry of the dendrimer and are found to be scattered around the dendrimer surface [15], see Figure 4. One can

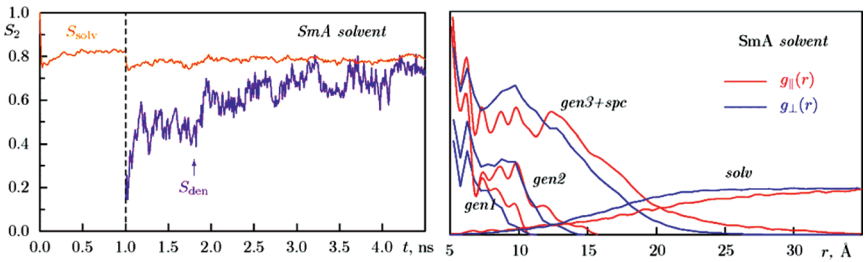

FIGURE 3 Relaxation of LCDr mesogens order parameter S_{den}, left (S_{solv} is the order parameter for the solvent) and RDFs for different generations of dendrimer and for the solvent, right (*gen1-gen3* denote generations, *spc* denotes terminal spacers and *solv* denote solvent, the signs $\parallel$ and $\perp$ indicate RDF in directions parallel and perpendicular to solvent director), model A, smectic A solvent.

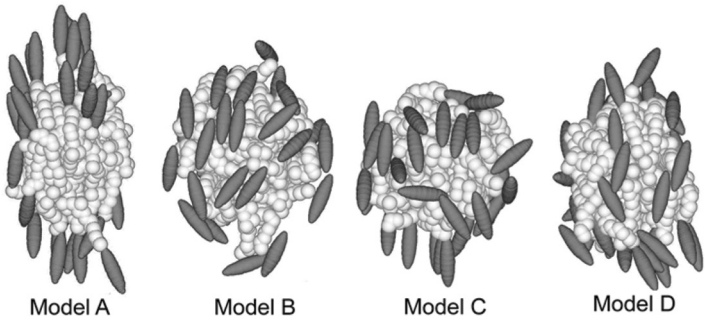

FIGURE 4 Snapshots showing the shape of model A–D LCDrs in a nematic solvent, (polymer sites of the dendritic scaffold and of terminal spacers are shown as spheres, while the mesogens are shown as ellipsoids).

suggest that realignment of the laterally attached beads involves much stronger deformation of the dendritic core and for decoupling of these two subsystems much longer terminal spacer is needed. Clarification of this point will need additional studies. For models C and D a mixed effect is observed. The terminally bonded mesogens are able to migrate to the ends of the dendrimer to form partial rods, with the remaining laterally bonded groups scattered over the dendrimer surface [15]. We expect this change in shape to have a major influence in determining the packing of molecules in the bulk and the consequently the mesophases they can form.

3. STRUCTURE AND INTERNAL DYNAMICS OF SIDE CHAIN LIQUID CRYSTALLINE POLYMER IN VARIOUS PHASES

Side-chain LC polymers (SCLCPs) have already found applications for optical data storage, for manufacturing diffractive elements, in addition to other areas [16]. Experimental studies concentrate mostly on their liquid crystallinity (as seen in phase diagrams), optical properties and some details of internal structure. Most of research has concentrated on the properties of the LC parts of the molecule, whereas the structure and properties of the polymeric subsystem has found less coverage [17]. The latter, however, is of considerable interest, too, as it is relevant to the mechanical properties, relaxation processes and processability of the material. One of the advantages of MD simulations is the ability to trace the position and velocity of each atom, hence, the arrangement of each SCLCP subsystems (backbones, mesogens and spacers) can be traced independently in any particular LC phase.

MD simulations of SCLCP are performed on two models, with chemical structures as shown in Figure 5, left. For model 1 [18], an array of 64 identical polymer molecules were placed in a simulation box and preliminary simulations were undertaken to relax the polymer configurations at 600 K. On cooling from this fully isotropic polymer melt, spontaneous microphase separation occurs into polymer-rich and mesogen-rich regions. Upon application of a small aligning potential during cooling, the structures that form on microphase separation anneal to produce a smectic-A phase in which the polymer backbone is largely confined between the smectic layers. Several independent quenches from the melt are described that vary in the strength of the aligning potential and the degree of cooling. In each quench, defects were found where the backbone chains hop from one backbone-rich region to the next by "tunnelling" through the mesogenic layers. The number of such defects is found to depend strongly on the rate of cooling. In the vicinity of such a defect, the smectic-A structure of the mesogen-rich layers is disrupted to give *nematic-like* ordering.

Additionally, several extensive annealing runs of approximately 40 ns duration have been carried out at the point of microphase separation. During annealing the polymer backbone is seen to be slowly excluded from the mesogenic layers and lie perpendicular to the smectic-A director. These observations agree with previous assumptions about the structure of a SCLCP and with interpretations of x-ray diffraction and small angle neutron scattering data.

For model 2 [19] with longer spacers (where each molecule has a backbone of 39 beads and ten side chains attached to it in syndiotactic way, see Fig. 5, right) the same basic behavior was observed. Here, a slightly different method for growing the smectic phase was employed.

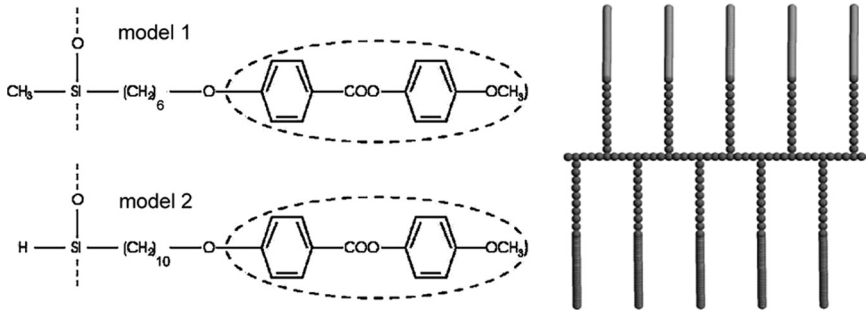

FIGURE 5 Chemical structures for models of SCLCPs used in MD simulations (left) and schematic representation of one molecule in model 2, right (beads represent polymer atoms, sticks show mesogens).

External fields of various strength were applied to the isotropic phase just below the smectic-isotropic transition temperature $T_{SI} \approx 490\,\mathrm{K}$. We found that in this way formation of defects is prevented (greater mobility aids the process of microphase segregation) but the stability of the smectic phase after the field is switched off depends crucially on the strength of the field being applied before. If the rearrangement of the mesogens takes place on a much faster scale than those for the polymer chains, the melt returns back to the isotropic phase. The bulk arrangement of the mesogens, side chain spacers and backbones is the same as for the model 1 and has a tightly packed "sandwiched" structure, see Figure 6.

We found that both the backbones and side chains keep their metric properties (derived from the gyration tensor) unchanged in isotropic, polydomain- and monodomain smectic A phases (see [19] for more details). This opens up the possibility for coarse grained simulations, where both backbones and side chains are replaced by certain soft elongated bodies. In our study we found that in the smectic A phase the order parameter of the mesogens was approximately 0.7, and that for the equivalent ellipsoids of side chains is about 0.4. Backbone equivalent ellipsoids are ordered within the layers to which backbones are confined (see Fig. 6), the order parameter is approximately 0.28 and the director is perpendicular to that for the mesogens.

Interesting transformations of the diffusion coefficient anisotropy are observed in the process of growing the smectic phase with the aid of an external field. During the initial growth phase, the diffusion of all components (backbones, side chains and mesogens) is much higher along the field, showing massive rearrangements in the melt. Thereafter, the situation is reversed and at the end of the smectic

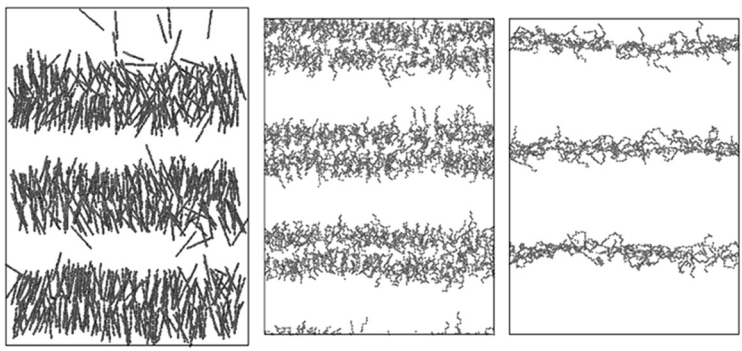

FIGURE 6 Arrangement of the mesogens (left), side chains (middle) and backbones (right) in the smectic A phase.

phase formation, diffusion along the field is effectively frozen out, showing one-dimensional 'solidification' of the smectic A phase. The diffusion coefficient in other directions is found to be essentially the same as in the polydomain smectic phase at the same temperature $T = 485\,\mathrm{K}$ [19].

4. SIMULATIONS OF PHOTO-INDUCED DEFORMATIONS IN AZOBENZENE-CONTAINING POLYMERS

Incorporation of azobenzene chromophores into polymer systems via covalent bonding or by blending gives rise to a number of unusual effects under visible and ultraviolet irradiation. While light-induced reorientation of azobenzene chromophores in the polymer matrix is now considered to be a well-understood process, the light-induced changes of the matrix itself have been a puzzling phenomenon. A satisfying explanation represents a great challenge for the azobenzene community and upon solving will definitely become a milestone in development of modern polymer physics. The most astonishing effect is the inscription of surface relief gratings (SRGs) onto thin azobenzene polymer films [20]. It is usually produced by exposing the sample to periodic intensity or a polarization pattern resulting from the interference of two polarized laser beams. The absorption of light at a wavelength of about 480 nm induces material flow even at room temperature, several tens of Kelvin below the glass transition temperature, *Tg*, of the polymers.

Another interesting and related effect is the photoinduced deformation of azobenzene polymer (referred thereafter as azo-polymer) films floating on a water surface [21]. It is demonstrated that different types of azobenzene side-chain polyesters undergo an "opposite change" of shape under illumination with linearly polarized light. Amorphous polyester (with a stiff main chain and a short spacer in the side chains) elongates along the direction of the electric field vector, while LC polyester (with a flexible main chain and a long spacer) contracts in the same direction [21]. This result is in agreement with the observation that the phase of the SRGs, relative to that of the optical grating, strongly depends on the chemical architecture of the particular azo-polymer. Hence, both spatially uniform and periodically modulated cases can be explained in terms of local deformations in the polymer film under illumination, namely, the local compressions occur in LC systems and the opposite effect of local extension takes place for amorphous azo-polymer. Therefore, in our modeling we consider small cuboidal boxes in '*dark*' and '*bright*' areas and study their possible anisotropic deformations under illuminated light.

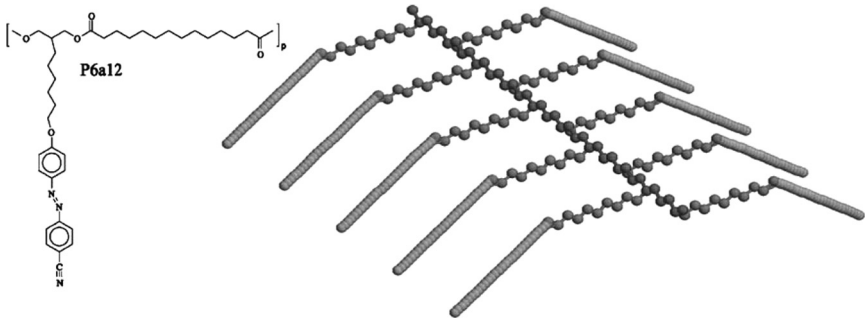

FIGURE 7 Weakly-coupled model, which represents the LC azo-polymer P6a12.

To describe the principle differences between the chemical structures of the LC and amorphous azo-polymers, we consider two characteristic topologies. Both are of the side-chain type but differ in terms of both backbone rigidity and in the degree of coupling between the backbone and the chromophores: hence the names "weakly" and "strongly coupled" models. The weakly-coupled [22] model has a flexible, alkyl-like backbone and relatively long flexible spacers of 10 pseudo-atoms. In contrast, the strongly-coupled model, has a very short spacer of 2 sites and both the backbone and the spacer are made relatively rigid by increasing the barriers for torsional interactions. Both topologies have the same backbone length of 39 pseudo-atoms and the same number of 10 side chains attached in a syndiotactic way. The relevant prototypes for these models are the P6a12 and E1aP polymers studied in Ref. [21], see Figures 7, 8.

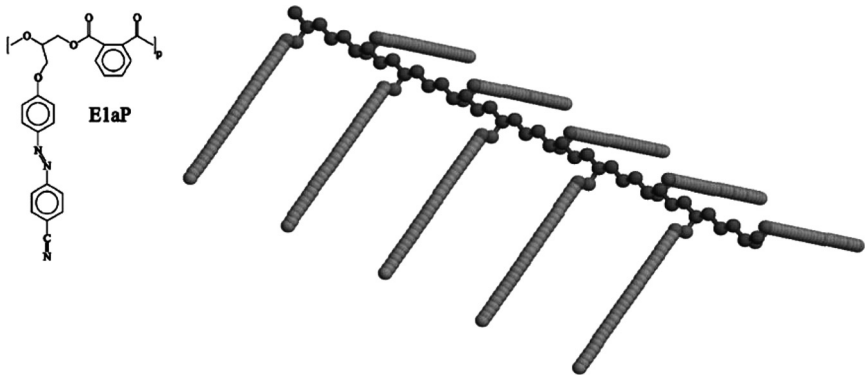

FIGURE 8 Strongly -coupled model, which represents the amorphous azo-polymer E1aP.

In this study we used the following parameterization for the Gay-Berne potential, $\mu = 1$, $\nu = 2$, length-to-breadth ratio $\kappa = 3$, side-to-side/end-to-end well depth ratio $\kappa' = 5$, the length and energy scale parameters are $\sigma_0 = 5$ Å and $\varepsilon_0 = 0.56127 \cdot 10^{-20}$ J. The MD simulations are performed in the $NP_{xx}\,P_{yy}\,P_{zz}T$ ensemble, where each component of the pressure $P_{\alpha\alpha}$ is controlled via separate Hoover barostats (for more details, see [19]). This allows anisotropic changes of the box dimensions to be monitored.

The photoisomerization of azobenzene is a complex quantum mechanical phenomenon, which involves excitation of the electrons of the N=N double bond and occurs on the time-scale of tens of picoseconds. However, from the perspective of our level of modeling, it can be considered as a classical mechanics perturbation that acts on azobenzenes and initiates further mechanical changes in the polymer structure. We assume that the material contains azobenzene with such chemical substituents that continuous cyclic *trans-cis* isomerization is possible under illumination and a photostationary state can be established. The *trans-cis* photoisomerization rate is known to be proportional to $\cos^2(\vartheta)$ (ϑ is the angle between the long axis of the isomer and the light polarization). Therefore in the photostationary state *trans* isomers are to be found predominantly perpendicular to the light polarization. This effect can be modeled by the existence of an imaginary field directed along the light polarization and introduced via an extra energy term in the system Hamiltonian, $U_i^{\text{field}} = \mathrm{F} \cdot P_2(\cos(\vartheta_i))$, where $F > 0$ and θ_I is an angle between the long axis of the θ_i *trans*-isomer and the direction of the field. We will use a reduced field strength, f, where $F = f \cdot 10^{-20}$ J, and $P_2(x) = (3x^2 - 1)/2$ is the second Legendre polynomial.

For the weakly-coupled model we analyzed the effect of the external field on the smectic A phase, which is build at $T = 485$ K (just below T_{SI}) following the method described in the previous section. The simulation box contained 64 molecules with a total number of 8896 polymer beads and 640 mesogens, the box dimensions were of the order of 100 Å. The direction of the field was chosen to be parallel to the mesogenic director (this corresponds to the experimental situation of a light beam hitting a polymer film with planar arrangement of mesogens). Two different scenarios are observed in weak ($f = 0.2$) and strong fields ($f = 1.5$). In weak fields, the only effect observed is a field-induced smectic-isotropic transition, see Figure 9, left. On the same time scale we observe contraction of the box along the field, due to repacking of the mesogens, see Figure 9, right. This effect is observed experimentally in nematic films under spatially modulated illumination when the film is examined by polarizing optical

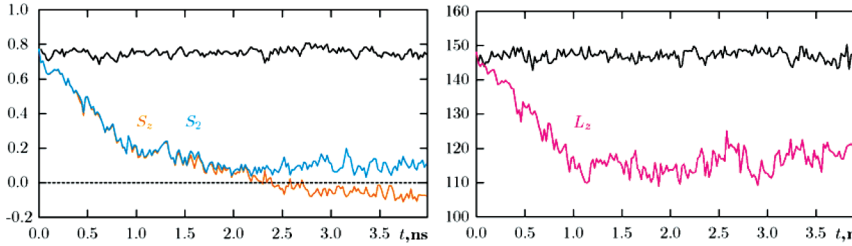

FIGURE 9 Order parameters (left) and box dimension along the field (right) evolution after applying a weak effective field, $f = 0.2$ (S_z is the order parameter along the field and S_2 is the usual nematic order parameter).

microscopy [23]. It also reproduces anisotropic shrinking of the P6a12 freely floating drop along the light polarization [21]. One should mention that the same effect would be observed in a polydomain film, but to a smaller extent, as only a fraction of chromophores will be repacked.

If the strength of the field increases, a second effect takes place, namely, the smectic phase is regrown with different spatial arrangement of the layers, where the mesogens are now positioned perpendicular to the field, see Figure 10. One should mention that shrinking of the polymer along the film takes place mainly due to smectic-isotropic (nematic-isotropic in other polymers) transition. In this respect, inclusion of the *cis*-isomer (these are not included in our study explicitly) will amplify this transition further.

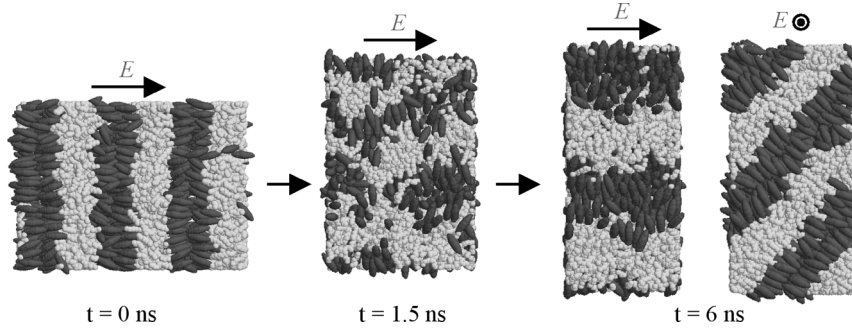

FIGURE 10 Snapshots that demonstrate field-induced sequence of phase changes in the strong field, $f = 1.5$, first smectic-isotropic transition and then isotropic-smectic transition with rearranged layers.

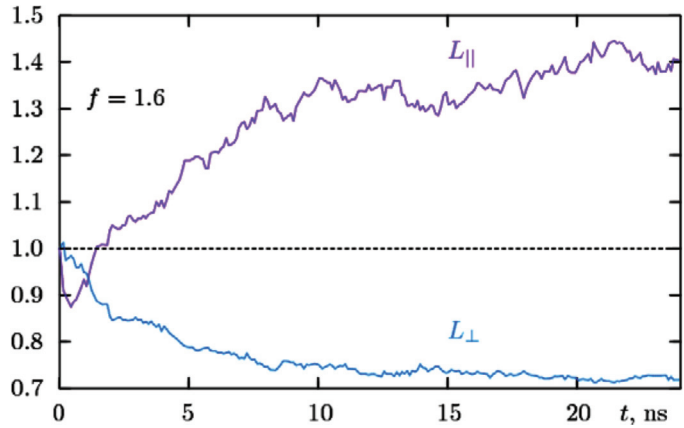

FIGURE 11 Scaled box dimension along the field, $L_{\|}$, and averaged box dimensions perpendicularly to it, $L_{\perp}$, strongly-coupled model, $f = 1.6$.

The strongly-coupled model does not exhibit a smectic phase. This is in agreement with typical experimental phase diagrams of SCLCPs with short spacers [24]. We studied the field-induced deformations of this model at $T = 485$ K, where the polymer is found in a polydomain phase. By applying the external field in certain interval of strengths, e.g., $f = 1.6$, at first some rapid contraction along the field is observed (similarly to the case of a weakly-coupled model), and then slower but substantial extension of the box takes place, see Figure 11. The effect is also observed on the snapshots of the melt, see Figure 12.

We found the following microscopic mechanism for this effect. The deformations of backbones is excluded as the metrics properties of these, monitored via semi-axes of their equivalent ellipsoids, are

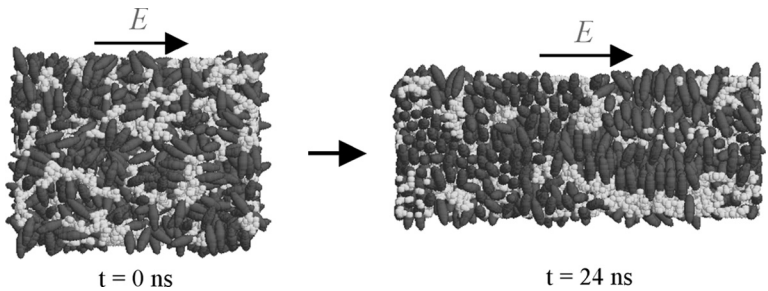

FIGURE 12 Snapshot for the field-induced extension of the sample, strongly-coupled model, $f = 1.6$.

unchanged (Fig. 13, left). Reorientation of the backbones happens on the same time scale as that for the mesogens (3–5 ns, see, Fig. 13, right), whereas the dimension of the box grows for at least another 5 ns (Fig. 13, right). Hence, the accumulated stress due to the repacking of the polymeric matrix is seen as the main driving force for the extension of the box. This is also confirmed by the fact that the box extends further for another 5 ns after the field is switched off. As in the case of the weakly coupled model, we should remark that the explicit existence

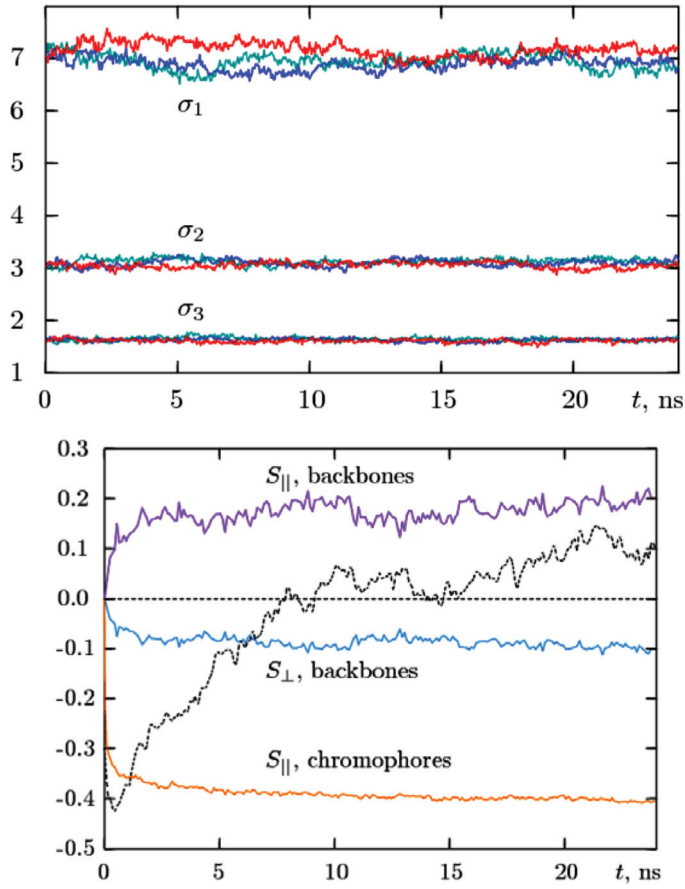

FIGURE 13 Semiaxes of the equivalent ellipsoids for the backbones (left) and order parameters for backbones and mesogens ordering (right). $S_{||}$ are the order parameters along the field whereas $S_{\perp}$ is the order parameter in the perpendicular direction, the black dashed line shows the reminder of the time scale for the extension of the box.

of the *cis*-isomers in the model will not change the above mentioned mechanism. To conclude, by constructing a strongly-coupled model we are able to reproduce the anisotropic deformation seen in free-floating amorphous polymers [21] by taking into account solely the reorientation of the *trans*-isomers of the chromophores.

5. CONCLUSIONS

We demonstrated that molecular dynamics simulations provide an extremely powerful technique for studying different properties of liquid crystalline polymers. Both solutions and melts are considered in this study and their internal structure and dynamics are analysed. The studies of macromolecules shape in various environments provide interesting pointers to the role played by molecular shape in the formation of supramolecular assemblies. For the azobenzene-containing polymers we suggested a classical mechanical mechanism which reproduces some aspects of photo-isomerization. By incorporation of this mechanism into molecular dynamics simulations, the opposite photo-induced deformations were obtained for liquid crystalline and amorphous polymers, reproducing experimental data.

REFERENCES

[1] Vogtle, F. (1993). *Supramolecular Chemistry: An Introduction*, Wiley: Chichester.
[2] Leach, A. R. (2001). *Molecular Modeling: Principles and Applications*, Pearson: Harlow.
[3] Frenkel, D. & Smit, B. (1996). *Understanding Molecular Simulation: From Algorithms to Applications*, Academic: San Diego.
[4] Wilson, M. R. (1997). *J. Chem. Phys.*, *107*, 8654.
[5] Wilson, M. R. (2007). *Chem. Soc. Rev.*, *36*, 1881.
[6] Allinger, N. L., Chen, K. S., & Lii, J. H. (1996). *J. Comp. Chem.*, *17*, 642.
[7] Glaser, M. A., Clark, N. A., Garcia, E., & Walba, D. M. (1997). *Spectrochimica Acta A*, *53*, 1325, D.L.G. Cheung, Ph.D. thesis, University of Durham, 2002.
[8] Matthews, O. A., Shipway, A. N., & Stoddart, J. F. (1998). *Progr. Polym. Sci.*, *23*, 1–56.
[9] Ponomarenko, S. A., Boiko, N. I., Shibaev, V. I., Richardson, R. M., Whitehouse, I. J., Rebrov, E. A., & Muzafarov, A. M. (2000). *Macromol.*, *33*, 5549–5558.
[10] Hughes, Z. E., Wilson, M. R., & Stimson, L. M. (2005). *Soft Matter*, *1*, 436.
[11] Vlugt, T. J. H., Krishna, R., & Smit, B. (1999). *J. Phys. Chem. B*, *103*, 1102.
[12] Gay, J. G. & Berne, B. J. (1981). *J. Chem. Phys.*, *74*, 3316.
[13] Ilnytskyi, J. & Wilson, M. R. (2001). *Comput. Phys. Commun.*, *134*, *23*; *ibid.*, *148*, 43.
[14] Wilson, M. R., Ilnytskyi, J. M., & Stimson, L. M. (2003). *J. Chem. Phys.*, *119*, 3509.
[15] Wilson, M. R., Stimson, L. M., & Ilnytskyi, J. M. (2006). *Liq. Cryst.*, *33*, 1167.
[16] Chung, T.-S. Ed. (2001). *Thermotropic Liquid Crystalline Polymers*, Technomic: Lancaster, PA.

[17] Dimitrova, A. (2000). Ph.D. thesis, University of Halle, Germany.
[18] Stimson, L. M. & Wilson, M. R. (2005). *J. Chem. Phys.*, *123*, 034908.
[19] Ilnytskyi, J. & Neher, D. (2007). *J. Chem. Phys.*, *126*, 174905.
[20] Rochon, P., Batalla, E., & Natansohn, A. (1995). *Appl. Phys. Lett.*, *66*, 136; Kim, D. Y., Tripathy, S. K., Li, L., & Kumar, J. (1995). *Appl. Phys. Lett.*, *66*, 1166.
[21] Bublitz, D., Helgert, M., Fleck, B., Wenke, L., Hvilstedt, S., & Ramanujam, P. S. (2000). *Appl. Phys. B*, *70*, 863.
[22] Ilnytskyi, J., Saphiannikova, M., & Neher, D. (2006). *Condens. Mat. Phys.*, *9*, 87.
[23] Yamamoto, T., Hasegawa, M., Kanazawa, A., Shiono, T., & Ikeda, T. (1999). *J. Phys. Chem. B*, *103*, 9873.
[24] Collings, P. J. & Hird, M. (2001). *Introduction to Liquid Crystals*, Taylor & Francis: London.